

MEASUREMENTS OF [O I] λ 6300/H α LINE INTENSITY RATIOS FOR FOUR O STAR H II REGIONS

N. R. HAUSEN, R. J. REYNOLDS, AND L. M. HAFFNER

Department of Astronomy, University of Wisconsin–Madison, 475 North Charter Street, Madison, WI 53706;
 hausen@astro.wisc.edu, reynolds@astro.wisc.edu, haffner@astro.wisc.edu

Received 2002 July 16; accepted 2002 September 4

ABSTRACT

We have used the Wisconsin H α Mapper facility to measure the [O I] λ 6300/H α line intensity ratios for four O star H II regions: S27 (observation coordinates $l = 6^\circ.3$, $b = +23^\circ.6$), S252 ($l = 190^\circ.1$, $b = +0^\circ.6$), S261 ($l = 194^\circ.1$, $b = -1^\circ.9$), and S264 ($l = 195^\circ.1$, $b = -12^\circ.0$). We find that the ratios range from 0.0015 to 0.0053. These results are roughly a factor of 10 lower than measured [O I]/H α ratios in directions that sample the warm ionized component of the interstellar medium. This difference implies a significantly lower hydrogen ionization ratio $n(\text{H}^+)/n(\text{H}^0)$ or higher electron temperature in the diffuse ionized gas compared with that in the bright discrete O star H II regions.

Key words: H II regions — ISM: clouds — ISM: general

1. INTRODUCTION

Reynolds et al. (1998) measured the [O I] λ 6300/H α line intensity ratio for one classical H II region, NGC 7000 (North America Nebula), and for three directions that sampled the much fainter diffuse interstellar medium. It was found that the [O I]/H α ratio for the H II region was roughly a factor of 10 below that in the diffuse background directions. The data for this paper were collected to investigate whether the [O I]/H α ratios of other discrete H II regions are of the same order of magnitude as that of NGC 7000. If so, it would imply a significant difference in the hydrogen ionization state or temperature between classical O star H II regions and the diffuse ionized gas.

2. OBSERVATIONS

The spectra for this paper were obtained using the Wisconsin H α Mapper (WHAM) facility located at Kitt Peak National Observatory. WHAM, designed to measure faint optical emission from diffuse interstellar gas, has a 1° beam on the sky and 12 km s^{-1} radial velocity resolution over a 200 km s^{-1} spectral range that can be centered on any wavelength between 4800 and 7300 Å. Additional information about WHAM and its operation is found in Tufté (1997) and Haffner (1999). The WHAM facility is remotely operable, and all data for this paper were gathered remotely from Madison, Wisconsin.

The observations were based on an “on-off” technique. An “on” exposure toward the desired H II region was immediately followed by an exposure toward an “off” direction approximately 10° away from the H II region. Subtracting the “off” spectrum from the “on” spectrum thus separates the H II region emission from the background emission. It also greatly reduces the intensity of atmospheric lines in the spectra, in particular the bright [O I] airglow line and the H α geocoronal line. This is important because the [O I] airglow line is typically 100–300 times brighter than the [O I] emission from the H II regions. To further separate the Galactic [O I] emission from the atmospheric emission, the observations were made during a time of the year when Earth’s orbital motion provided a significant Doppler shift between the terrestrial and interstellar [O I].

Table 1 provides a summary of the observations. The four O star H II regions were selected for study from a list of regions previously observed in H α and [S II] λ 6716 by Reynolds (1985, 1988). The brightness of these regions in H α indicated that the significantly fainter [O I] λ 6300 line could be clearly detected using exposures with a moderate amount of integration time. The exposure times listed in Table 1 are for the “on” spectra. Each “off” spectrum had the same amount of exposure time as the corresponding “on” spectrum. Except as noted in Table 1, each [O I] spectrum had an integration time of 300 s, and each H α spectrum had an integration time of 60 s. For region S27, the geocoronal line in the H α spectra and the airglow line in the [O I] spectra were positioned on the red side of the 200 km s^{-1} spectral range. In the spectra of the other regions, these atmospheric lines were positioned on the blue side of the spectral range.

3. RESULTS

Table 2 gives the results of the study, including the radial velocity and width of each of the [O I] and H α Galactic emission lines. The measured H α intensity averaged over the WHAM beam is also listed. The [O I] λ 6300/H α line intensity ratios shown in Table 2 include a correction for the slight differences in instrument response (optical transmittance and detector quantum efficiency) between 6300 and 6563 Å. The uncertainty in the ratios is dominated by the uncertainty in the intensity of the [O I] emission. Hence, the error bars on the line intensity ratios reflect only the uncertainty in the intensity of the [O I] emission components. Because of the large charge exchange cross section between oxygen and hydrogen in warm interstellar gas, the observed [O I]/H α line intensity ratio for a given direction can be used to calculate the ionization ratio of hydrogen $n(\text{H}^+)/n(\text{H}^0)$ within the emitting gas. From Reynolds et al. (1998) and references therein,

$$\frac{I_{[\text{O I}]}}{I_{\text{H}\alpha}} = 2.74 \times 10^4 \frac{T_4^{1.854}}{1 + 0.605 T_4^{1.105}} \exp\left(-\frac{2.284}{T_4}\right) \frac{n(\text{O})}{n(\text{H})} \times \frac{1 + n(\text{H}^+)/n(\text{H}^0)}{[1 + (8/9)n(\text{H}^+)/n(\text{H}^0)]n(\text{H}^+)/n(\text{H}^0)}, \quad (1)$$

TABLE 1
LIST OF OBSERVATIONS

REGION	IONIZING STAR (HD)	SPECTRAL TYPE ^a	OBSERVATION DIRECTION (<i>l</i> , <i>b</i>)	OBSERVATION DATE	TOTAL EXPOSURE TIME (s)	
					[O I] λ 6300	H α
S27.....	149757 (ζ Oph)	O9.0 V	6 $^{\circ}$ 3, +23 $^{\circ}$ 6	1999 Apr 16	1200 ^b	240 ^c
	1999 Apr 20	1200 ^b	240 ^c
S252.....	42088	O6.5 V	190 $^{\circ}$ 1, +0 $^{\circ}$ 6	1999 Feb 13	300	60
S261.....	41997	O7.5 V	194 $^{\circ}$ 1, -1 $^{\circ}$ 9	1999 Feb 13	300	60
S264.....	36861 (λ Ori)	O8.0 III	195 $^{\circ}$ 1, -12 $^{\circ}$ 0	1999 Feb 13	300	60

^a From Cruz-González et al. 1995, available at <http://cdsweb.u-strasbg.fr/viz-bin/VizieR?-source=III/84B>.

^b Individual spectra are 600 s exposures.

^c Individual spectra are 120 s exposures.

TABLE 2
RESULTS

REGION	[O I] λ 6300		H α			$I([\text{O I}])/I(\text{H}\alpha)$ (Energy Units)	$n(\text{H}^+)/n(\text{H}^0)$	
	V_{LSR} (km s $^{-1}$)	FWHM (km s $^{-1}$)	V_{LSR} (km s $^{-1}$)	FWHM (km s $^{-1}$)	I (R)		6000 K	10,000 K
S27.....	-1 \pm 5	8 \pm 7	+2 \pm 1	21 \pm 1	77 \pm 2	0.0039 \pm 0.0021	16	160
S252.....	+5 \pm 1	11 \pm 3	+6 \pm 1	24 \pm 1	214 \pm 2 ^a	0.0039 \pm 0.0005	16	160
S261.....	+6 \pm 2	9 \pm 4	+5 \pm 1	22 \pm 1	71 \pm 1 ^a	0.0053 \pm 0.0013	12	120
S264.....	+12 \pm 3	8 \pm 5	+8 \pm 1	20 \pm 1	165 \pm 2	0.0015 \pm 0.0006	42	420

^a Because the region did not fill WHAM's 1 $^{\circ}$ beam, actual surface brightness is greater than the intensity value listed.

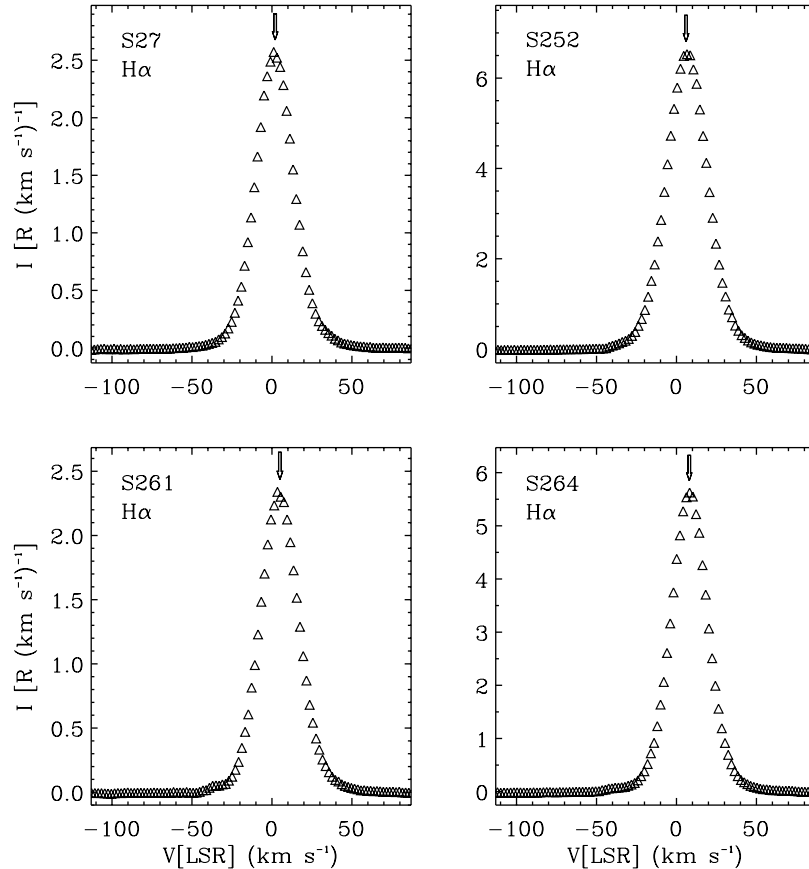


FIG. 1.—H α spectra toward the four H II regions. Each spectrum is an “on-off” subtraction representing 60 s of integration time toward the H II region. In each spectrum, an arrow marks the velocity of the H α emission. Residuals from the incompletely subtracted H α geocoronal line are near -40 km s $^{-1}$ in the S252, S261, and S264 spectra. The spectrum for region S27 was produced using the data from 1999 April 16 only, and the geocoronal residuals are near +30 km s $^{-1}$. The intensity scale for all four spectra is R (km s $^{-1}$) $^{-1}$, and in each case a constant was subtracted from the spectrum to bring the background level to zero.

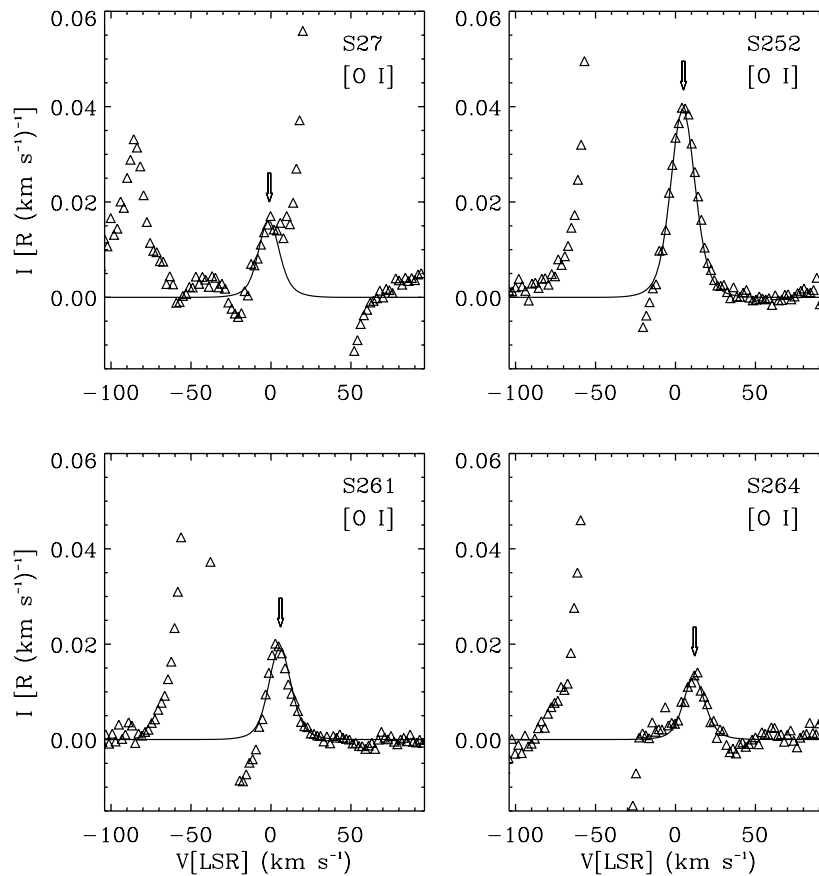


FIG. 2.—[O I] $\lambda 6300$ spectra toward the four H II regions. Each spectrum is an “on-off” subtraction representing 300 s of integration time toward the H II region. The intensity scale for all four spectra is $R \text{ (km s}^{-1}\text{)}^{-1}$, and in each case a constant was subtracted from the spectrum to bring the background level to zero. The Gaussian fit (solid line) in each spectrum models the parameters for that H II region given in Table 2, and the arrow marks the velocity of the [O I] emission. The residuals from the incomplete subtraction of the [O I] airglow line are centered near -40 km s^{-1} in the spectra for regions S252, S261, and S264. The spectrum for region S27 was produced using the data from 1999 April 16 only and shows the [O I] airglow line residual centered near $+30 \text{ km s}^{-1}$, in addition to the subtraction residual of an OH airglow line at -85 km s^{-1} .

where $I_{[\text{O I}]} / I_{\text{H}\alpha}$ is the intensity ratio measured in energy units and T_4 is the electron temperature in units of 10^4 K . The factor $n(\text{O}) / n(\text{H})$ is the gas-phase abundance of oxygen, which we take to be 3.2×10^{-4} (Meyer, Jura, & Cardelli 1998). The final two columns in Table 2 list the hydrogen ionization ratios, which were calculated using equation (1) and two different electron temperatures, 6000 and 10,000 K.

Figure 1 presents the $\text{H}\alpha$ “on-off” spectra of the four H II regions, and Figure 2 gives the corresponding [O I] $\lambda 6300$ “on-off” spectra. As the spectra in Figure 2 show, baseline uncertainty resulting from the incomplete subtraction of terrestrial features, particularly the bright [O I] airglow line (see § 2), is the primary source of uncertainty in the [O I] spectra. The baseline uncertainty in the spectrum for region S27 is the most severe, and data for S27 were obtained on two separate dates (see Table 2) in an attempt to reduce this uncertainty. Data from both nights showed a weak feature near -40 km s^{-1} in addition to the nebular [O I] line near the LSR associated with the H II region (see Fig. 2). For the subsequent analysis, however, it was assumed that this weak feature is not associated with the S27 H II region.

4. DISCUSSION AND CONCLUSIONS

We have found that the [O I] $\lambda 6300 / \text{H}\alpha$ line intensity ratios for the four O star H II regions observed in this study range from 0.0015 to 0.0053. These values are of the same order of magnitude as [O I] / $\text{H}\alpha$ ratios observed in other H II regions. Specifically, Reynolds et al. (1998) measured 0.0033 for the [O I] / $\text{H}\alpha$ ratio in NGC 7000, which is ionized by an O6.0 V star (Shull & Van Steenberg 1985), and Osterbrock, Tran, & Veilleux (1992) observed an [O I] / $\text{H}\alpha$ ratio of 0.0033 for a region just north of the Trapezium in the Orion Nebula (O6.0 V).

These H II region results stand in contrast to measurements of [O I] / $\text{H}\alpha$ ratios in directions that sample the diffuse ionized background. For example, Reynolds et al. (1998) studied three such directions ($l = 114^\circ$, $b = 0^\circ$, $l = 130^\circ$, $b = 0^\circ$, and $l = 130^\circ$, $b = -7.5^\circ$) and found [O I] / $\text{H}\alpha$ ratios of 0.020, 0.028, and 0.044, respectively, for the emission components associated with diffuse ionized gas in the Perseus spiral arm near -40 km s^{-1} and placed an upper limit of 0.012 on the [O I] / $\text{H}\alpha$ ratio for an emission component toward $(130^\circ, -7.5^\circ)$ near -60 km s^{-1} . In addition, Hausen

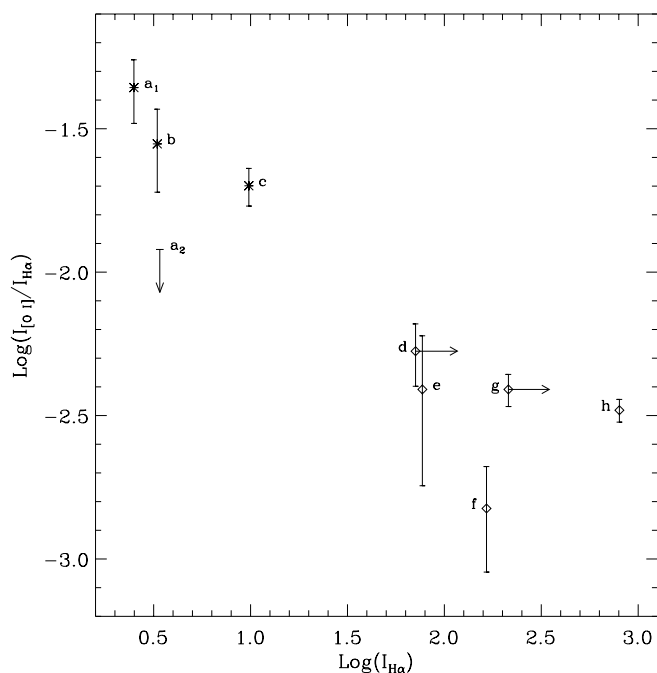


FIG. 3.—[O I] $\lambda 6300/\text{H}\alpha$ line intensity ratio plotted versus the $\text{H}\alpha$ intensity within the WHAM beam for five H II regions and three diffuse background directions. The labels (a)–(h) indicate directions and regions as follows: a₁, $l = 130^\circ$, $b = -7.5$ (emission component at -31 km s^{-1}); a₂, $l = 130^\circ$, $b = -7.5$ (emission component at -60 km s^{-1}); b, $l = 130^\circ$, $b = 0^\circ$; c, $l = 114^\circ$, $b = 0^\circ$; d, S261; e, S27; f, S264; g, S252; h, NGC 7000. For labels a–c, which correspond to diffuse background directions, the measured [O I]/ $\text{H}\alpha$ ratio in each case is marked with a star (except for a₂, for which only an upper limit on the ratio was determined). Error bars are also shown for a₁, b, and c. For labels d–h, which correspond to H II regions, the measured ratio in each case is marked with a diamond flanked by error bars. The arrows associated with d and g indicate that the surface brightness of the regions is an undetermined amount greater than the plotted value because the region does not fill WHAM’s beam (see Table 2). Data for d–g are given in Table 2, and data for a–c and h are from Reynolds et al. (1998).

et al. (2002) observed the high-latitude ($b = +62^\circ$) line of sight toward HD 93521 and determined an upper limit of 0.43 for the [O I]/ $\text{H}\alpha$ ratio corresponding to emission near -50 km s^{-1} , with one possible fit to the data yielding the value 0.18 for the ratio. Similar [O I]/ $\text{H}\alpha$ ratios have been reported for the diffuse ionized gas in other galaxies (e.g., Rand 1998). Hence, on average, the ratios for the classical H II regions are an order of magnitude lower than those for the diffuse background directions.

Incorporating the data in Table 2 with data from Reynolds et al. (1998), Figure 3 is a plot of [O I]/ $\text{H}\alpha$ ratios ver-

sus $\text{H}\alpha$ intensity for five H II regions and three directions that sample the diffuse ionized gas. As Figure 3 shows, this sample of H II regions does not indicate any dramatic variation in [O I]/ $\text{H}\alpha$, even though the regions exhibit a wide range of $\text{H}\alpha$ surface brightnesses and spectral types of the ionizing stars. The ratios for regions S27, S252, and S261 are mutually consistent to within the estimated uncertainties, while the ratio for NGC 7000 is likewise consistent (to within the uncertainties) with the ratios for S27 and S252 and is only slightly lower than that for S261. The ratio for S264 is noticeably lower than the other H II region ratios, but it is still within 2σ of the ratio for S27.

The large difference in [O I]/ $\text{H}\alpha$ ratios between the H II regions and the diffuse background directions is illustrated in Figure 3. The average [O I]/ $\text{H}\alpha$ ratio is 0.0036 for the H II regions, while the average ratio is 0.031 for the diffuse emission components near -40 km s^{-1} in the Perseus arm (see above). From equation (1), we can see that a difference such as this could be due to a significantly lower hydrogen ionization ratio $n(\text{H}^+)/n(\text{H}^0)$ or to a higher electron temperature in the diffuse ionized gas compared with the H II regions. A temperature of about 7000–8000 K for the H II regions is consistent with the widths of the $\text{H}\alpha$, [O I], and [S II] emission lines (e.g., Reynolds 1988). If, for example, both the H II regions and the diffuse gas have a temperature of 8000 K, then equation (1) yields $n(\text{H}^+)/n(\text{H}^0) = 71$ [or $n(\text{H}^+)/n(\text{H}_{\text{total}}) = 0.99$] for the H II regions and $n(\text{H}^+)/n(\text{H}^0) = 8$ [or $n(\text{H}^+)/n(\text{H}_{\text{total}}) = 0.89$] for the diffuse ionized gas. Alternatively, a similar calculation can be done assuming that $n(\text{H}^+)/n(\text{H}^0)$, rather than temperature, is constant between the H II regions and the diffuse background directions. If a temperature of 8000 K (or 7000 K) is adopted for the H II regions, then a temperature of approximately 15,000 K (or 12,000 K) is required for the diffuse ionized gas. There is, in fact, evidence of elevated temperatures in the diffuse gas compared with the H II regions (see, e.g., Reynolds et al. 2001; Haffner, Reynolds, & Tufte 1999; Reynolds, Haffner, & Tufte 1999), but this evidence does not indicate temperatures as high as 12,000–15,000 K. Therefore, the large difference between [O I]/ $\text{H}\alpha$ ratios in H II regions and the diffuse ionized background is more likely due to a combination of a higher temperature and a lower hydrogen ionization fraction within the diffuse gas.

We thank Trudy Tilleman for providing night-sky condition reports from Kitt Peak during the observations. This work and the operation of WHAM were supported by the National Science Foundation through grant AST 96-19424.

REFERENCES

- Cruz-González, C., Recillas-Cruz, E., Costero, R., Peimbert, M., & Torres-Peimbert, S. 1995, VizieR On-Line Data Catalog (Garching: Max-Planck-Institut für extraterrestrische Physik), III/84B
Haffner, L. M. 1999, Ph.D. thesis, Univ. Wisconsin Madison
Haffner, L. M., Reynolds, R. J., & Tufte, S. L. 1999, *ApJ*, 523, 223
Hausen, N. R., Reynolds, R. J., Haffner, L. M., & Tufte, S. L. 2002, *ApJ*, 565, 1060
Meyer, D. M., Jura, M., & Cardelli, J. A. 1998, *ApJ*, 493, 222
Osterbrock, D. E., Tran, H. D., & Veilleux, S. 1992, *ApJ*, 389, 305
Rand, R. J. 1998, *ApJ*, 501, 137
Reynolds, R. J. 1985, *ApJ*, 294, 256
———. 1988, *ApJ*, 333, 341
Reynolds, R. J., Haffner, L. M., & Tufte, S. L. 1999, *ApJ*, 525, L21
Reynolds, R. J., Hausen, N. R., Tufte, S. L., & Haffner, L. M. 1998, *ApJ*, 494, L99
Reynolds, R. J., Sterling, N. C., Haffner, L. M., & Tufte, S. L. 2001, *ApJ*, 548, L221
Shull, J. M., & Van Steenberg, M. E. 1985, *ApJ*, 294, 599
Tufte, S. L. 1997, Ph.D. thesis, Univ. Wisconsin Madison